

SINERGI Vol. 29, No. 3, October 2025: 845-856 http://publikasi.mercubuana.ac.id/index.php/sinergi http://doi.org/10.22441/sinergi.2025.3.024



Evaluation of recycled steel properties originating from construction steel waste



Mohamad Zarif Mirza Alias, Nur Ezzaryn Asnawi Subki, Hazrina Mansor*, Yazmin Sahol Hamid, Nurizzati Hidayah Mohd Afendi, Mazlan Mohd Yusoff, Ellvera De Ermalina Dominic, Nur Saihah Nasurudin

Faculty of Civil Engineering, Universiti Teknologi MARA (UiTM) Shah Alam, Malaysia

Abstract

This research presents an experiment of constructional recycled steel properties that has been remelted into component-shaped specimens using green sand casting. A series of tensile, compressive and toughness tests were conducted. Then, specimens were observed using Scanning Electron Microscopy (SEM) and Energy-Dispersive X-ray (EDX) for microstructure analysis and chemical composition determination. This experiment was done to determine whether the recycled steel quality met the industrial standards. All tests were conducted at Universiti Teknologi MARA (UiTM), providing data on the stress-strain relationship and toughness of recycled steel. The results indicated that recycled steel exhibited tensile characteristics below the standard strength range required by Eurocode. The changes in Young's modulus of the steel were attributed to exposure to high temperatures, causing significant vibration within the steel atoms and increasing the distance between atoms, thereby reducing tensile strength. The influence of impurities may also be a factor affecting tensile strength. The tests also concluded that the recycled steel construction waste was a brittle material with an average V-notch toughness of 24J.

This is an open-access article under the CC BY-SA license.



Keywords:

Experimental test; Metallurgical; Recycled steel;

Article History:

Received: October 15, 2024 Revised: March 20, 2025 Accepted: July 24, 2025 Published: September 5, 2025

Corresponding Author:

Faculty of Civil Engineering, Universiti Teknologi MARA (UiTM) Shah Alam, Malaysia Email:

hazrina4476@uitm.edu.my

INTRODUCTION

Steel is the most recycled material globally, with approximately 680 million metric tons of recycled scrap recorded in 2021 [1]. Recycled products typically originate from a combination of pre- and post-consumer scrap sources [2], which can be a challenge. Generally, three common approaches can be utilized in the steel production industry: Blast Furnace (BF), Direct Reduced Iron (DRI), and Electric Arc Furnace (EAF) [3, 4, 5, 6]. EAF is notably more aligned with the production of steel, offering lower carbon emissions [3, 4, 5], in line with the Sustainable Development Goal (SDG). EAF, essentially using electricity to heat metal to a soft state for shaping, requires input materials that are already reduced, which means the process does not directly produce steel from iron ore [1][7]. Moreover, this EAF approach can be integrated

with a hydrogen-based process, known as "fossil-free steelmaking" [8]. Conversely, BF technology (73% utilization) in steelmaking uses coke as a reducing agent and provides heat for the iron ore reduction process [5]. While the DRI method uses fossil carbon-based fuels as the reductant [9]. It involves the utilization of natural gas as both fuel and reductant for the iron ore reduction process in a shaft furnace [5][10]. This method can also be integrated into the EAF process as (DRI-EAF) to replace the traditional BF [11].

Currently, secondary steel constitutes merely 30% of global steel production [4][9]. Therefore, the EAF production technique via recycled steel serves as a crucial input required for all steelmaking process routes for the future [3]. Hence, expanding the proportion of total steel production derived from secondary sources presents a notable opportunity to mitigate CO₂

emissions from the iron and steel sector [4]. This can be achieved, in part, by augmenting the portion of end-of-life (EOL) scrap that undergoes recycling.

Bringing the concept of recycling steel into fruition to reduce CO2 emissions is not a straightforward task [2, 12, 13]. As indicated in a study cited by [14], there is an inadequate supply of scrap to fulfill the global economy's steel demand [4][9]. This shortage jeopardizes steel recycling for high-grade applications. Danny in 2021 [15], categorized three types of scrap by steel lifespan, namely: (1) forming scrap, generated during the casting and shaping of intermediate steel such as rods, tubes, and sheets; (2) fabrication scrap, resulting from the cutting of intermediate products into final products; and (3) end-of-life (EOL) scrap, coming from fullyutilized products that have reached their service life. Currently, steel scraps are graded mainly by visual inspection, human interference, and decision, which contribute to issues related to safety and accuracy of grading [16]. This leads to difficulties in processing secondary steel [17][18].

Steel recycling can degrade steel products quality [15][19]. In some cases, the alloying elements found in steel scraps are difficult to separate [20]. Melting a mixture of different alloys can result in an unstable composition due to microstructural inhomogeneity. For example, studies on high-entropy and multi-component alloys show that both simulations and experiments yield two-phase or multi-phase mixtures after melting, rather than a uniform solid solution [21][22]. Additionally, small quantities of non-steel contaminants such as plastic, copper wire, or aluminum are often mixed in due to imperfect separation of materials before melting [20]. While some impurities can be vaporized or removed as slag during melting or refining, others may remain or not be sufficiently eliminated [23].

Recent research conducted by [23], introduces a novel oxysulfide electrolyte for electrorefining that significantly improves steel recycling by efficiently eliminating carbon and copper impurities from molten iron. This electrolyte leverages sulfide that is specifically used for copper extraction, resulting from high ionic conductivity with the dilution of molten oxide. This ground-breaking process also produces liquid iron and sulfur as by-products, which potentially reduce emissions and solve issues in secondary steel production.

Castro et al. [24] have developed a matrix illustrating which combinations of contaminants and metals in the EAF input mix should be avoided. Two primary considerations are to be

determined, including the feasibility of eliminating the contaminant from the primary metal during the refining process and the separation of the contaminant from the dust or slag economically. According to Castro et al. [24] findings, aluminum and magnesium mixed with steel must be avoided, while copper, platinum-group metals, stainless steel, and zinc mixed with steel are recommended to be avoided. Other researchers concerning impurity content and it consequences generated from building constructions (which are commonly contaminated by copper wire) [25], end the life of vehicle (which is the most significant source of contaminants) [26, 27, 28, 29], Mechanical equipment [30], Steel in packaging [31] (with a very thin layer of tin or of chromium and chromium oxide that is retained within the melted steel) has been well reported.

Extensive research and literature have been conducted to assess the effect of different manufacturing processes on steel properties, such as the hot dipping aluminizing effect [32], the heat rate with the austenitization temperature effect [33], and the effect of corrosion on steel properties [34]. Kateusz et al. [35] conducted an experiment to investigate the influence of recycled stainless-steel coatings from mixed scraps under thermal exposures.

However, research on determining mechanical properties such tensile, as compressive, flexural, and impact strength of recycled steel that is produced by a sustainable method (e.g., EAF) has proven to be limited. Therefore, further research is essential to investigate the mechanical properties of recycled steel scrap and identify the properties of steel waste after it has been remelted and recycled. This research aims to conduct a study to assess the mechanical properties, metallurgical, and chemical composition of recycled steel waste used in construction.

METHOD

The experiment was conducted in phases from Phase 1 to Phase 4.

Phase 1: Collection and Preparation

Two distinct types of construction steel waste were collected from the waste disposal site at the Heavy Structure Laboratory, College of Engineering, Universiti Teknologi MARA (UiTM) Shah Alam, which included discarded corrugated reinforcement bars with unknown steel grade, featuring a diameter of 12 mm, as well as British Reinforced Concrete (BRC) steel meshes.



Figure 1. Collected construction steel waste

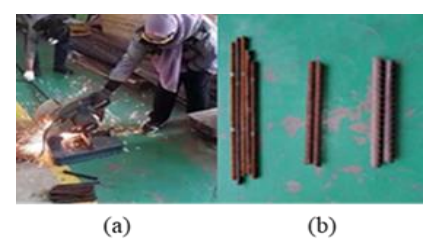


Figure 2. (a) Cutting process and (b) smaller pieces of steel waste

Although the collected materials were originally used for reinforcement, it was categorized as steel waste due to their defects. Cleaning the collected steel waste is important to remove any unwanted particles, such as rust. Then, a visual inspection was performed for initial quality assessment. Figure 1 illustrates the collected construction steel waste. The total weight of collected materials was about 93 kg. The collected construction steel waste was cut into smaller pieces to suit different testing and fit into the small opening size of the Electric Arc Furnace (EAF), which is 40 cm in diameter. In addition, reducing the size of the reinforcement bars also provided better thermal conductivity due to a higher surface-to-volume ratio, which will help to reduce the energy required in the melting process.

Figure 2(a) shows the cutting process of the collected construction steel waste into smaller pieces using a metal cut-off grinder. Figure 2(b) shows the smaller pieces of BRC steel meshes (left), and reinforcement bars (middle and right). Before the steel waste can be melted, the mold that will be used for casting the molten steel must be prepared.

Phase 2: Pattern Making and Molding

Pattern making is typically done using materials made from metal or wood. In this study, the patterns replicating the final product of the cast material were first prepared using plywood and wooden sticks. The plywood was cut into a dimension of 300 mm x 200 mm with a thickness of 16 mm, replicating a final product of a solid

rectangular steel plate (see Figure 3(a)). The plywood edges were chamfered to ease the removal work. Then, three similar wooden sticks (see Figure 3(b)) were cut into a length of 75 mm with a diameter of 25 mm that replicates the final product of solid cylindrical steel in compliance with ASTM E9-19 [36].

The sand-molding method was utilized to produce the recycled steel specimen. A sand mold, as shown in Figure 4, was created using green sand, which is composed primarily of sand and clay, and an adequate amount of moisture to facilitate binding effects. The preparation of the sand mold involved two parts: the drag (bottom flask) and the cope (top flask), as depicted in Figure 4.

The drag flask was prepared as indicated in Figure 5(a) by first placing the plywood pattern at the bottom of the flask and then adding the green sand. The green sand surrounding the plywood design was firmly compacted with a hand rammer until it was strong enough to form a cavity wall that could sustain the pattern when it was removed. When compacting green sand, it is crucial to keep the pattern in place and proceed with caution to avoid trapping air bubbles in the mold during pouring, which could result in blow defects. Subsequently, the drag flask was inverted, and the plywood pattern was carefully removed. Two runners were created next to the mold cavity, as seen in Figure 5(b). These runners connect the pouring sprue and riser to the mold cavity (refer to Figure 4). Two conical tubes, which would function as the pouring sprue and the riser (see Figure 4) were positioned appropriately before the green

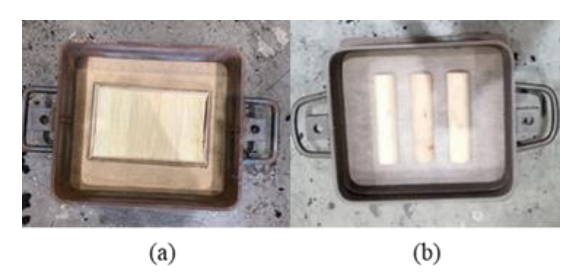


Figure 3. (a) A plywood and (b) a wooden stick pattern

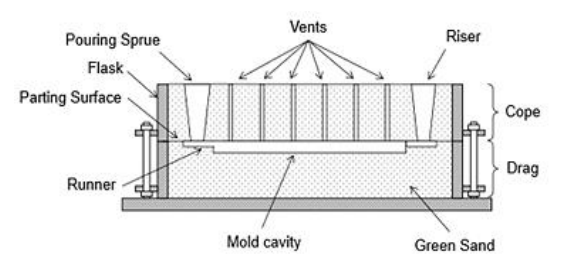


Figure 4. Sand-molding components

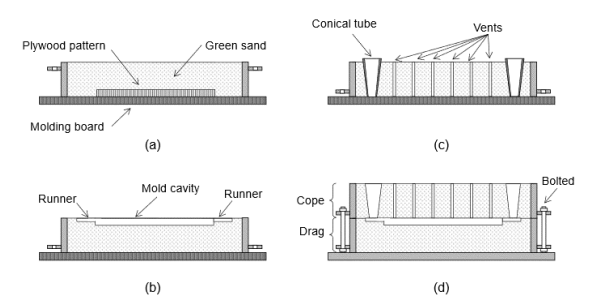


Figure 5. Construction of sand mold: (a)
Preparation of sand mold in drag flask, (b)
constructing runners beside the mold cavity, (c)
preparation of sand mold in cope flask, and (d)
complete construction of sand mold.

sand was poured into the cope flask (refer to Figure 5(c)). Vents, or ventilation holes, were made by penetrating steel rods all the way through the cope flask, as shown in Figure 5(c). This will let air circulate more easily during pouring. After the green sand was thoroughly compacted, the conical tubes were carefully removed. The cope flask was then gently positioned atop the drag flask and tightened with bolts to provide stability (see Figure 5(d)). To enable the green sand to consolidate even further, the sand mold was left for a day. Similar steps (refer to Figure 5) were repeated by replacing the plywood with three wooden stick patterns for solid cylindrical steel products in a mold.

Phase 3: Melting and Casting

The melting process of construction steel waste was conducted at the Foundry Laboratory, College of Engineering, Universiti Teknologi MARA (UiTM) Shah Alam, using the Electric Arc Furnace (EAF), as shown in Figure 6(a). The temperature of the furnace was raised to 1550 °C. which is the melting point of steel. The melting process was carried out in batches, using about 45 kg of construction steel waste in each batch. To aid in the melting process, 15 kg of steel scrap were fed into the furnace as it was gradually heated to the required temperature. Once the molten steel was visible, the furnace was gradually filled with construction steel waste (see Figure 6(b)). Simultaneously, ferrosilicon was added to improve the fluidity of molten steel, which in turn made casting easier. 200g of carbon riser was also added to the furnace during the casting process to increase its carbon content, which reduced the steel porosity. During the melting process, slag coagulant was consistently introduced into the furnace to separate impurities and non-metallic compounds from the molten steel. This resulted in the formation of slag

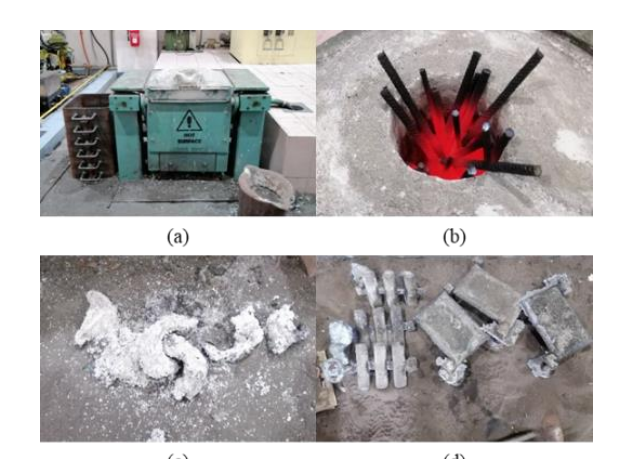


Figure 6. (a) Electric Arc Furnace, (b) construction steel waste in the furnace, (c) slag particles formation, and (d) recycled steel after cooling

particles, as shown in Figure 6(c), which were then removed from the furnace.

The molten steel was kept at 1545 °C for a few hours before it was poured into two different mold shapes: One for a solid rectangular plate and the other for a solid cylindrical mold that had been prepared earlier. The molten steel was left for 24 hours at room temperature to allow for cooling and solidification before the mold could be opened.

After 24 hours from casting, the recycled steel specimens were shaken out of the sand mold for the sand shot blasting process, whereby any remaining sand was removed from the recycled steel specimens. Figure 6(d) shows the recycled steel specimens after they were removed from the sand molds. The recycled steel specimens, involving rectangular- and cylindrical-shaped specimens, then underwent finishing processes, which involved the removal of excess steel components (such as risers and runners), cutting the connections between the specimens, and polishing of the steel surfaces using a grinder. A solid rectangular steel plate and three solid cylindrical steel plates were ready for the testing process. Subsequently, three (3) steel specimens were extracted from the solid rectangular steel plate through waterjet cutting to get the desired shape, while milling and grinding to achieve the necessary thickness.

Phase 4: Experimental Testing

Three (3) mechanical tests were conducted, including the uniaxial tensile, uniaxial compression, and Charpy Impact test to determine the mechanical behavior of the recycled steel specimen under different stress states. Also, the recycled steel specimen was observed using

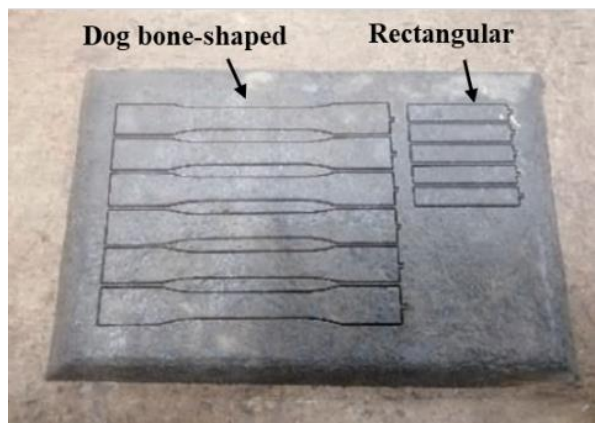


Figure 7. Dog bone-shaped specimens for the tensile test and rectangular specimens for the toughness test

Scanning Electron Microscope (SEM) to analyze the microstructure of recycled steel and Energy Dispersive X-ray (EDX) to assess the chemical composition of recycled steel.

For the uniaxial tensile test, three (3) dog bone-shaped specimens were cut from the solid rectangular steel plate (refer to Figure 7) and designated as ST1, ST2 and ST3. The sampling method and uniaxial tensile test procedure were conducted in accordance with ISO6892-1:2019 [37]. The dimensions of a tensile test specimen can be seen in Figure 8. This test was performed using the Universal Testing Machine (UTM). The strain rate control testing method, also known as Method A2 in ISO6892-1:2019 [37], was employed with a single strain rate approach. This approach is suitable for determining various key parameters such as yield strength, fracture strength, and others. The tensile test was executed in a quasi-static manner at a constant loading rate of 0.025mm/s with ±20% tolerance.

On the other hand, three (3) solid cylindrical specimens were lathed for better surface finishing and prepared for the uniaxial compression tests, such as SC1, SC2, and SC3. The procedures for conducting a uniaxial compression test, including specimen preparation, were referred to as ASTM E9-19 [36].

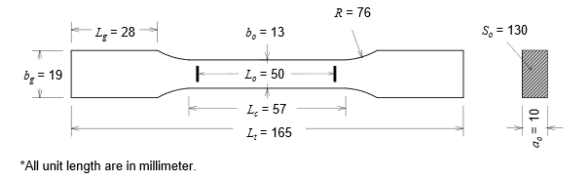
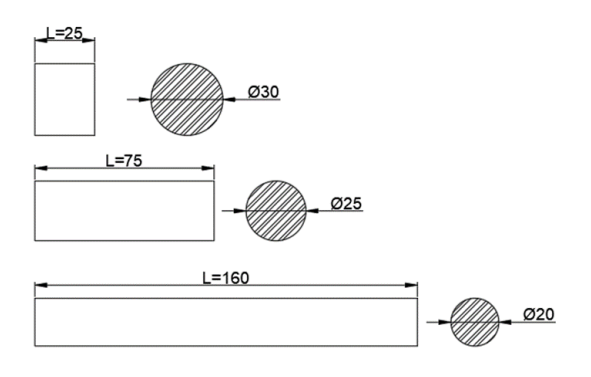


Figure 8. Dimension of a dog bone-shaped tensile specimen in accordance with BS EN ISO6892-1:2019 [37].



*All unit length are in millimeter.

Figure 9. Dimension of solid cylindrical compressive test specimen in accordance with ASTM E9-19 [36].

Based on the standard, short specimens are generally utilized for compression tests of bearing metals. Medium-length specimens are usually used for establishing the general compressive strength properties of metals. Long specimens are best suited for determining the elastic modulus in compression of metals. Specimens with an L/D (length/diameter ratio) of 1.5 or 2.0 are best suited for determining the compressive strength of high-strength materials. This test was conducted mainly to determine the general compressive strength of recycled steel. Thus, only a medium-length design was selected for the compressive test specimens. The dimensions of solid cylindrical steel specimens can be seen in Figure 9.

Then, three (3) rectangular specimens were extracted from the solid rectangular steel plate (refer to Figure 7) for the Charpy Impact test, with each specimen designated as SI1, SI2, and SI3. This test was conducted to assess the toughness of recycled steel specimens. Material toughness quantifies the maximum amount of energy that a material can absorb before it fractures, which is helpful to determine whether a material is ductile or brittle. The sampling method and test procedure were conducted in compliance with ISO148-[38]. Detailed dimensions 1:2016 of the rectangular specimen with the presence of Vnotch can be seen in Figure 10. The test was executed using the impact testing machine which consists of a pendulum hammer and a scale measuring energy. The Charpy impact test procedure involves releasing the pendulum hammer from a state of free fall until it contacts the sample, causing it to break. The energy required to break the sample essentially represents the toughness of steel material, which is commonly expressed as the impact strength (i.e. energy per

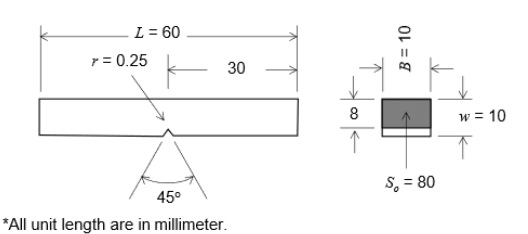


Figure 10. Dimension of rectangular specimen with V-notch

unit area of the notch). Note that the energy capacity of the testing machine was 300J.

Then, a specimen with dimensions of 10 mm x 10 mm and a maximum thickness of 40 mm was cut from the solid rectangular plate using an angle grinder. This recycled steel specimen was placed under a Scanning Electron Microscope (SEM) for microstructural observation. The specimen preparation and operating procedures were conducted in compliance with ASTM E3-11:2017 [39]. Image outputs were observed at different magnifications, including 1000x and 5000x.

In conjunction with SEM analysis, Energy Dispersive X-ray analysis was performed to determine the chemical composition of the recycled steel specimen. A high energy electron beam in a range of 10 to 20 keV was bombarded on the specimen, and X-rays emitted from the specimen were collected by an energy dispersive spectrometer. The energy of the X-rays generated represents characteristics of the atomic structure of elements from which it is emitted and hence presents the elemental details of the recycled steel specimen. For comparison, the chemical composition of the collected construction steel was identified by using a handheld X-ray Fluorescence (XRF) before going through the melting process.

RESULTS AND DISCUSSION

Results of tensile, compressive and toughness tests were presented and discussed in this section.

Tensile Properties of Recycled Steel

The uniaxial tensile test results of recycled steel originating from construction steel waste were presented in Figure 11 and summarized in Table 1 The initial stiffness of recycled steel specimens, or known as the Young's modulus, was estimated to be E = 2583 MPa on average, given in Table 1.

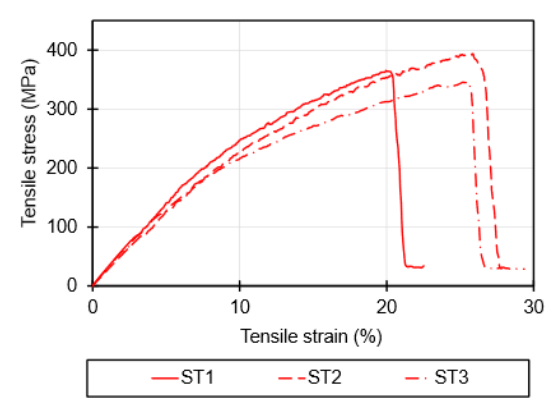


Figure 11. Tensile stress-strain properties of the recycled steel specimen.

The Young's modulus of the recycled steel specimen was significantly lower than mild steel (i.e. E = 210 GPa), but quite comparable to the commonly adopted strain hardening stiffness of mild steel (i.e. $E_{sh} = 0.01E = 2100$ MPa) as specified in EN1993-1-5:2006 [40]. The changes in Young's modulus of the steel were attributed to high temperature exposure, causing significant vibration within the steel atoms and increasing the distance between atoms, thereby reducing tensile strength.

As shown in Figure 11, the initial stiffness of the recycled steel specimen dropped after surpassing the proof yield strength at $f_{y,0.2}$ = 194.8 MPa on average (see Table 1). The post-yielding stiffness of the recycled steel material, also known as strain hardening stiffness, was estimated to be E_{sh} = 988 MPa on average (see Table 1). Essentially, the initial stiffness of the recycled steel specimen declined by 38% on average (i.e., E_{sh} = 0.38E). As given in Table 1, the recycled steel specimen fractures at the nominal strain of ε = 24.0% with an average fracture strength of f_f = 354.9 MPa. The significant drop in stiffness, which is also called stiffness degradation, occurred due to the microstructural changes during recycling processes, including melting and casting. It can be seen in Figure 12 that the steel was oxidized throughout the melting process, with abundance of ferric oxides observed under SEM.

The presence of pores and voids is also contributing to lower steel strength and density. Without the addition of 200g of carbon riser and 300g of ferrosilicon as catalysts, the steel porosity will be higher, which can make the steel even weaker. The idea of carbon riser addition was to ensure that the carbon is uniformly distributed throughout the molten steel and increase its strength, while the addition of ferrosilicon was to remove unwanted oxides and reduce the porosity of steel.

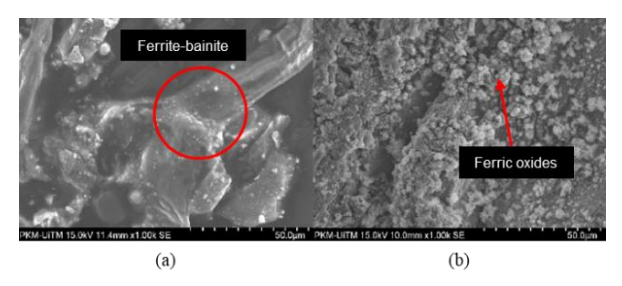


Figure 12. SEM images of (a) raw reinforcement bar, and (b) recycled steel specimen under 50μm magnification.

Table 1. Summary of key parameters on the tensile behavior of recycled steel specimens

Specimen	ST1	ST2	ST3	Average
Young's modulus, <i>E</i> (MPa)	2721	2450	2580	2583
Strain hardening stiffness, <i>E_{sh}</i> (MPa)	1150	980	835	988
Proof yield strength, f _{y,0.2} (MPa)	208.0	195.4	181.0	194.8
Fracture strength, <i>f_f</i> (MPa)	349.5	377.6	337.6	354.9
Proof, yield strain, $\varepsilon_{y,0.2}$ (%)	8.0	8.2	7.5	7.9
Fracture strain, $\varepsilon_f(\%)$	20.4	25.9	25.6	24.0

Besides, decarburization occurs during the steel melting process with the presence of oxygen or hydrogen, as steel loses carbon atoms, hence, reduced in strength and toughness (refer to (1)). This is also related to the impurities, such as rust that are rich in oxygen. Rust or iron oxides can combine with other elements in the steel to form other metallic compounds, thus weakening the steel.

$$FeO + C = Fe + CO \tag{1}$$

This can be seen through the XRF and EDX results of raw construction steel and recycled steel specimens, respectively, as in Figure 13 which presents the elemental details of raw construction steel and recycled steel specimens. percentage of carbon atoms in raw construction steel was higher compared to that carbon atoms in the recycled steel specimen. This proves that removal carbon atoms the of through decarburization has occurred in the steel melting process. The optimum amount of carbon for mild steel is typically between 0.05% and 0.25%. But the carbon content of the recycled steel specimen was 1.6%. This shows that the addition of a carbon riser was inappropriate for molten steel during the melting process. In comparison to mild steel that is commonly used in the steel industry, the yield and ultimate strength of recycled steel are significantly lower than mild steel, as in Table 2.

Compressive Properties of Recycled Steel

The compressive test results of recycled steel originating from construction steel waste were presented in Figure 14 and summarized in Table 3. The compressive strength of the recycled steel specimen was found to be 183.87 MPa on average. Due to high porosity, the compressive strength of the recycled steel specimen was notably lower than mild steel (i.e. f_u = 250 MPa). Based on the 0.2% plastic strain, the recycled steel specimen SCM-1 has a yield strength value of 47.758 MPa, specimen SC-2 was 38.803 MPa, while SC-3 was 43.28 MPa.

Toughness of Recycled Steel

The results of the Charpy Impact test are summarized in Table 4. Assuming that the energy loss due to friction was negligible, the average energy loss due to breakage of the V-notch specimen was KV = 24J (Refer Table 4). The failure mechanism of V-notch specimens involved the splitting of the specimens into two pieces, which is commonly referred to as the cleavage fracture. The surface fracture exhibited a shiny look with a combination of white and grey hues. The visual examination of the specimens confirms that the recycled steel specimen exhibited brittleness, which further supports the findings of the monotonic tensile test.

Table 2. Comparison of recycled steel specimens to mild steels available in the industry

Specimen	Young's Modulus (GPa)	Yield Strength (MPa)	Ultimate Strength (MPa)
Recycled steel	2.583	194.8	354.9
S275 [41]	210	275	430
Reclaimed steel by wall-saw cutting [42]	211.1	286	463.8
Reclaimed steel by wire-saw cutting [42]	210.7	279.3	461.2

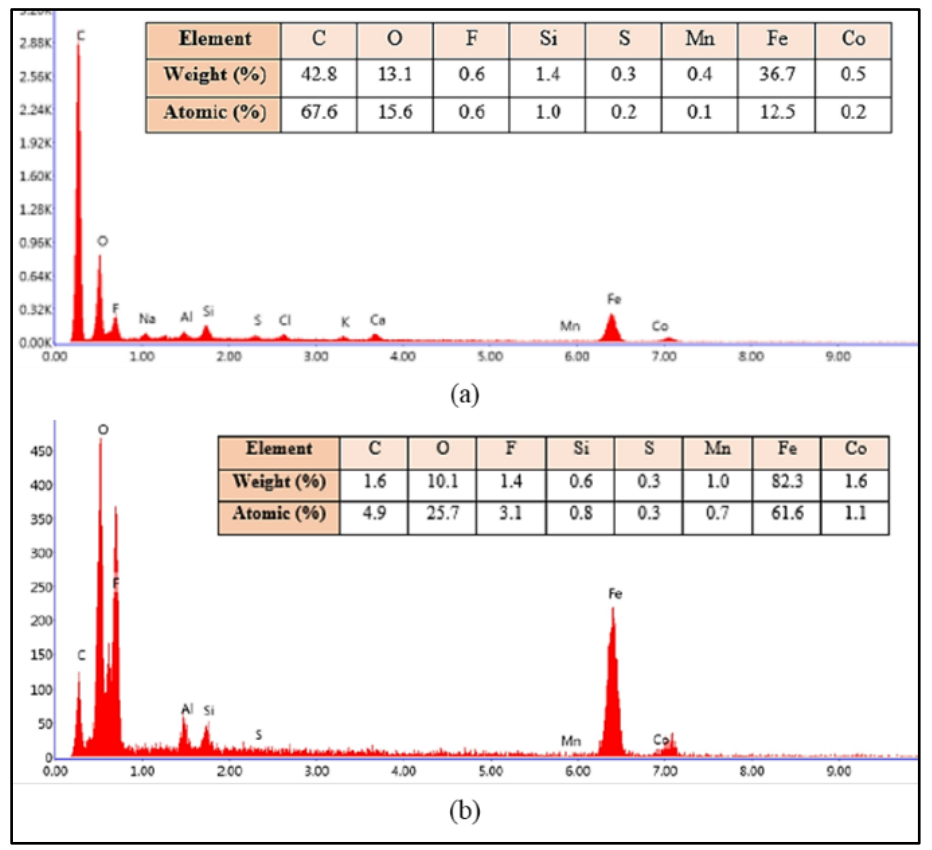


Figure 13. Elemental details of: (a) raw construction steel using handled XRF, and (b) recycled steel specimen using EDX analysis

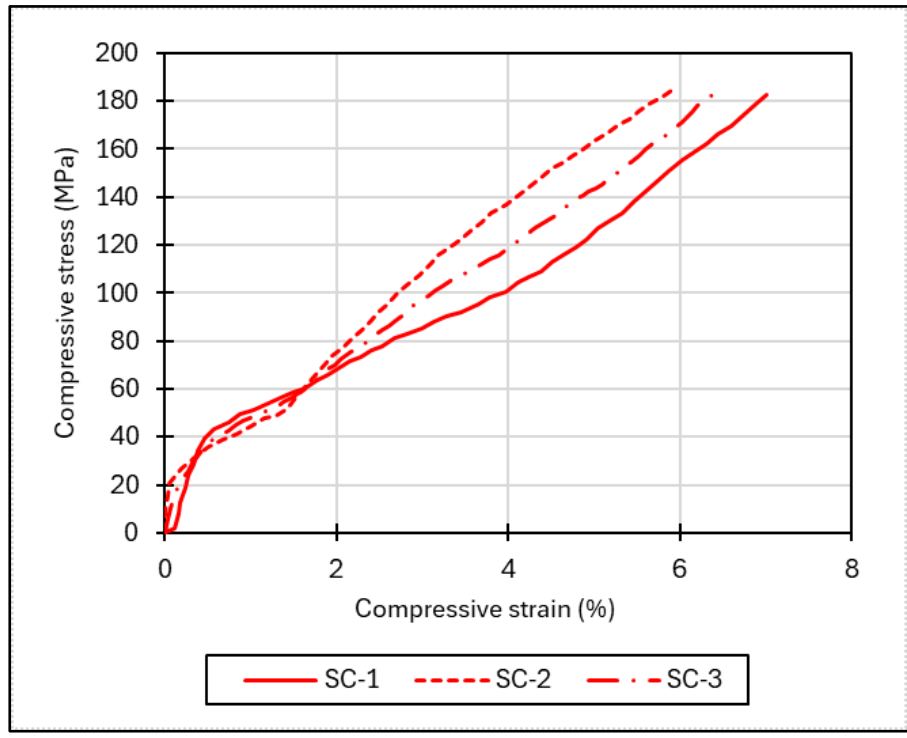


Figure 14. Compressive stress-strain of the recycled steel specimen

Table 3. Summary of key parameters on compressive properties of the recycled steel

specimens SC2 SC3 Specimen SC1 Average Ultimate Compressive 183.1 185.205 183.3 183.87 Strength, f_u (MPa) Yield Compressive 47 76 38.803 43.28 43.28 Strength, fy (MPa)

Table 4. Key parameters on impact strength of the recycled steel specimens.

and recycled electropechniches.				
Specimen	SI1	SI2	SI3	Average
Energy				
loss due				
to	32	22	20	24
breakage,				
KV (J)				
Impact				
strength	0.4	0.38	0.25	0.31
(J/mm ²)				

Table 5. Comparison of impact strength of the recycled steel specimens to S275JR grade mild steel at room temperature (20°C).

Specimen	Energy loss due to breakage, KV (J)	Impact strength (J/mm²)
Recycled steel	24	0.31
S275JR [38][43]	27	0.34

In comparison (Refer Table 5), a typical impact strength of an S275 grade mild steel is 0.34 J/mm², which is slightly higher than the recycled steel specimen. This may be due to the density difference between recycled steel and S275JR mild steel. A lower impact strength indicates that the recycled steel has poor toughness and is more susceptible to brittle fracture under impact loading conditions. Several possible causes of its low impact strength include the presence of impurities and the inappropriate rapid cooling rate of molten steel after the melting process. Thus, the recycled steel specimen cannot be used for applications where a minimum of S275JR is specified.

CONCLUSION

In summary, the study successfully achieved its objectives. Based on the findings, it is evident that none of the recycled steel specimens met the requirements for conventional steel grades. All the test specimens exhibited brittle behavior under different stress states, which are characterized by brittle fracture without any visible necking before reaching the fracture point. This behavior could be attributed to the presence of voids that lead to high porosity, the residual

impurities are not totally removed such as rust, and the decarburization of steel during melting process which has reduced the carbon content of remelted steel as proven through SEM and EDX analyses. In terms of toughness, the tested specimens demonstrated an average energy loss of KeV 24J due to the breakage of V-notch specimens, with the V-notch specimens splitting into two pieces, indicating an expected cleavage fracture.

These findings suggest a significant deviation from the standards of conventional steel grades. Therefore, the output from this study highlights the need for further improvement in future research. For future investigations, it is essential to segregate the quality of the recycled steel waste used according to its sources. Additionally, to prevent defects such as porosity, voids, and the formation of honeycomb, an optimum amount of carbon riser and ferrosilicon should be added during the melting process. Precautionary steps during melting and casting, such as setting the holding temperature above the flow point, can help prevent impurities in the finished product. Finally, enhancing the number of samples tested and sorting them according to the category of recycled steel waste would further enhance the validity of the research. Finally, it is beneficial if a network of advanced steel recycling facilities in Malaysia is equipped with technologies for refining and enhancing the quality of recycled steel to meet industry standards while developing a guideline to ensure uniformity in dealing with steel recycling.

ACKNOWLEDGMENT

The Authors would like to thank Universiti Teknologi MARA (UiTM) for their facilities and experts in completing this research successfully, and Geran Insentif Penyeliaan (GIP) for financial support to the author throughout this research period.

REFERENCES

- [1] Worldsteel Association, "Fact sheet: Steel and raw materials," World Steel Association, Brussels, 2023.
- [2] M. Venkataraman, Z. Csereklyei, E. Aisbett, A. Rahbari, F. Jotzo, M. Lord and J. Pye, "Zero-carbon steel production: The opportunities and role for Australia," *Energy Policy*, vol. 163, no. 0301-4215, p. 112811, April 2022, doi: 10.1016/j.enpol.2022.112811
- [3] H. Gao, J. Liu and I. Daigo, "Methodology development for estimating the impact of restriction factors to promote national steel recycling," *Resources, Conservation &*

- Recycling, vol. 215, April 2025, doi: 10.1016/j.resconrec.2024.108052
- [4] J. Suer, M. Traverso and N. Jager, "Review of Life Cycle Assessments for Steel and Environmental Analysis of Future Steel Production Scenarios," *Sustainability*, vol. 14, no. 21, p. 14131, 2022, doi: 10.3390/su142114131
- [5] M. Shahabuddin, G. Brooks and M. A. Rhamdhani, "Decarbonisation and hydrogen integration of steel industries: Recent development, challenges and technoeconomic analysis," *Journal of Cleaner Production*, vol. 395, p. 136391, April 2023, doi: 10.1016/j.jclepro.2023.136391.
- [6] H. Xin, S. Wang, T. Chun, X. Xue, W. Long, R. Xue and R. Zhang, "Effective pathways for energy conservation and emission reduction in iron and steel industry towards peaking carbon emissions in China: Case study of Henan," *Journal of Cleaner Production*, vol. 399, p. 136637, 2023, doi: 10.1016/i.jclepro.2023.136637
- [7] J. Shen, Q. Zhang and S. Tian, "Decarbonization pathways analysis and recommendations in the green steel supply chain of a typical steel end user-automotive industry," *Applied Energy*, vol. 377, no. Part-D, p. 124711, 1 January 2025, doi: 10.1016/j.apenergy.2024.124711
- [8] C. Richardson-Barlow, A. J. Pimm, P. G. Taylor and W. F. Gale, "Policy and pricing barriers to steel industry decarbonisation: A UK case study," *Energy Policy*, vol. 168, p. 113100, September 2022, doi: 10.1016/j.enpol.2022.113100
- [9] M. Rumsa, M. John and W. Biswas, "Global steel decarbonisation roadmaps: Near-zero by 2050," *Environmental Impact Assessment Review*, vol. 112, p. 107807, 2025, doi: 10.1016/j.eiar.2025.107807
- [10] Y. Wang, J. Liu, X. Tang, Y. Wang, H. An and H. Yi, "Decarbonization pathways of China's iron and steel industry toward carbon neutrality," *Resources, Conservation and Recycling*, vol. 194, p. 106994, July 2023, doi: 10.1016/j.resconrec.2023.106994
- [11] S. Speizer, S. Durga, N. Blahut, M. Charles, J. Lehne, J. Edmonds and S. Yu, "Rapid implementation of mitigation measures can facilitate decarbonization of the global steel sector in 1.5°C-consistent pathways," *One Earth*, vol. 6, no. 11, pp. 1494-1509, 17 November 2023, doi: 10.1016/j.oneear.2023.10.016
- [12] J.-S. Ludger Bernsmann and J. H. Schleifenbaum, "From construction for

- construction: Additive manufacturing with gas-atomized recycled steel scrap," *Circular Economy*, vol. 4, no. 3, ID: 100157, September 2025, doi: 10.1016/j.cec.2025. 100157
- [13] B. Kazmi, S. A. Taqvi and D. Juchelkova, "State-of-the-art review on the steel decarbonization technologies based on process system engineering perspective," *Fuel*, vol. 347, p. 128459, September 2023, doi: 10.1016/j.fuel.2023.128459
- [14] P. W. Griffin and G. P. Hammond, "The prospects for 'green steel' making in a netzero economy: A UK perspective," *Global Transition,* vol. 3, pp. 72-86, 2021, doi: 10.1016/j.glt.2021.03.001
- [15] L. D. Danny Harvey, "Iron and steel recycling: Review, conceptual model, irreducible mining requirements, and energy implications," Renewable and Sustainable Energy Reviews, vol. 138, p. 110553, 2021, doi: 10.1016/j.rser.2020.110553
- [16] W. Xu, P. Xiao, L. Zhu, Y. Zhang, J. Chang, R. Zhu and Y. Xu, "Classification and rating of steel scrap using deep learning," Engineering Applications of Artificial Intelligence, vol. 123, p. 106241, 2023, doi: 10.1016/j.engappai.2023.106241
- [17] D. K. Sainy, A. K. Saraf and N. S. Rathee, "Potential of metals recovery from end-of-life," in *Materials Today: Proceedings*, 2023, doi: 10.1016/j.matpr.2023.03.001
- [18] N. Kostwein, C. Kickinger, O. Glushko and R. Schnitzer, "Tracking changes in segregation on a single grain boundary in a ferritic steel by repeated atom probe tomography," *Journal of Materials Research and Technology*, vol. 38, pp. 4908-4916, 2025, doi: 10.1016/j.jmrt.2025.08.260
- [19] D. Panasiuk, I. Daigo, T. Hoshino, H. Hayashi, E. Yamasue, D. H. Tran, B. Sprecher, F. Shi and V. Shatokha, "International comparison of impurities mixing and accumulation in steel scrap," *Journal of Industrial Ecology*, vol. 26, pp. 1040-1050, 2022, doi: 10.1111/jiec.13246
- [20] J. Cejka, B. Sammer, I. Gruber, G. Klosch and S. K. Michelic, "Influence of Tramp Elements on Surface Properties of Liquid Medium-Carbon Steels," *Steel Research International*, vol. 95, no. 8, p. 2300715, 25 June 2024, doi: 10.1002/srin.202300715
- [21] C. J. Parker, K. Zuraiqi, V. Krishnamurthi, E. L. Mayes, P. H. A. Vaillant, S. S. Fatima, K. Matuszek, J. Tang, K. Kalantar-Zadeh, N. Meftahi, C. F. McConville, A. Elbourne, S. P. Russo, A. J. Christofferson, K. Chiang and T.

- Daeneke, "Spontaneous Liquefaction of Solid Metal-Liquid Metal Interfaces in Colloidal Binary Alloys," *Advanced Science*, vol. 11, no. 2400147, pp. 1-9, 2024, doi: 10.1002/advs.202400147
- [22] M. Moussa, S. Gorsse, . J. Huot and J. L. Bobet, "Effect of the Synthesis Route on the Microstructure of HfxTi(1-x)NbVZr Refractory High-Entropy Alloys," *Metals*, vol. 13, p. 343, 2023, doi: 10.3390/met13020343
- [23] J. Paeng, W. D. Judge and G. Azimi, "Electrorefining for copper tramp element removal from molten iron for green steelmaking," *Resources, Conservation and Recycling*, vol. 206, no. 0921-3449, p. 107654, July 2024, doi: 10.1016/j.resconrec.2024.107654
- [24] M. B. G. Castro, J. A. M. Remmerswaal, M. A. Reuter and U. J. M. Boin, "A thermodynamic approach to the compatibility of materials combinations for recycling," *Resources, Conservation and Recycling*, vol. 43, no. 1, pp. 1 19, 2004, doi: 10.1016/j.resconrec.2004.04.011
- [25] E. Yamasue, R. Minamino, H. Tanikawa, I. Daigo, H. Okumura, K. N. Ishihara and P. H. Brunner, "Quality evaluation of steel, aluminum, and road material recycled from end-of-life urban buildings in Japan in terms of total material requirement," *Journal of Industrial Ecology*, vol. 17, no. 4, pp. 555 565, 2013, doi: 10.1111/jiec.12014
- [26] K. E. Daehn, A. C. Serrenho and J. M. Allwood, "How will copper contamination constrain future global steel recycling?," Environmental Science and Technology, vol. 51, no. 11, p. 6599–6606, 2017.
- [27] H. Ohno, K. Matsubae, K. Nakajima, Y. Kondo, S. Nakamura and T. Nagasaka, "Toward the efficient recycling of alloying elements from end of life vehicle steel scrap," *Resources, Conservation and Recycling*, vol. 100, pp. 11 20, 2015, doi: 10.1016/j.resconrec.2015.04.001
- [28] H. Ohno, K. Matsubae, K. Nakajima, S. Nakamura and T. Nagasaka, "Unintentional flow of alloying elements in steel during recycling of end-of-life vehicles," *Journal of Industrial Ecology*, vol. 18, no. 2, pp. 242 253, 2015, doi: 10.1111/jiec.12095
- [29] H. Ohno, K. Matsubae, K. Nakajima, Y. Kondo, S. Nakamura, Y. Fukushima and T. Nagasaka, "Optimal recycling of steel scrap and alloying elements: Input-output based linear programming method with its application to end-of-life vehicles in Japan," *Enviromental Science and Technology*, vol.

- 51, no. 22, pp. 13086 13094, 2017, doi: 10.1021/acs.est.7b04477
- [30] H. Hatayama, I. Daigo and K. Tahara, "Tracking effective measures for closed-loop recycling of automobile steel in China," *Resources, Conservation and Recycling*, vol. 87, pp. 65 - 71, 2014, doi: 10.1016/j.resconrec.2014.03.006
- [31] E. Bluett, J. Edy, M. Dodd, A. de Vooys, N. Wint, E. Jewell and H. McMurray, "The influence of chromium oxide coating weight on filiform corrosion of trivalent chromium coatings for packaging steel," *Electrochimica Acta*, no. 523, 20 May 2025, doi: /10.1016/j.electacta.2025.145943
- [32] D. Prayitno and A. A. Abdunnaafi, "Effect of hot dipping aluminizing on the toughness of low carbon steel," *SINERGI*, vol. 25, no. 1, pp. 75-80, February 2021, doi: 10.22441/sinergi.2021.1.010
- [33] H. Wahyudi, S. E. Pratiwi, A. A. Supriyanto and D. P. Bayyu Aji, "The influence of heat rate and austenitization temperature on microstructure and hardness of Hadfield steel," *SINERGI*, vol. 27, no. 2, pp. 241-248, June 2023, doi: 10.22441/sinergi.2023.2.012
- [34] F. Fahimuddin, M. Kasmuri, R. Sofyan, S. Junaidi and L. MS, "Effect of one-year corrosion on steel bridge materials in the maintenance stage with the Charpy impact test method," *SINERGI*, vol. 27, no. 2, pp. 153-162, June 2023, doi: 10.22441/sinergi.2023.2.002
- [35] F. Kateusz, A. Polkowska, K. Chat-Wilk, K. Chrzan, D. Serafin, S. Pawlik, T. Dudziak and J. Jedlinski, "Steam oxidation of thermally deposited coatings from 304 L and recycled 316 L/Z100 steels: Influence of temperature, coatings microstructure and steel recycling," Surface and Coatings Technology, vol. 494, no. 2, p. 131478, 2024, doi: 10.1016/j.surfcoat.2024.131478
- [36] ASTM E9-19, "Standard Test Methods for Compression Testing of Metallic Materials at Room Temperature," ASTM International, 2019.
- [37] BS EN ISO 6892-1:2019, "Metallic materials Tensile testing Part 1: Method of test at room temperature," International Organization for Standardization, London, 2019.
- [38] BS EN ISO 148-1:2016, "Metallic materials Charpy pendulum impact test Part 1: Test method," International Organization for Standardization, 2016.

- [39] ASTM E3-11:2017, "Standard Guide for Preparation of Metallographic Specimens," ASTM International, United States, 2017.
- [40] BS EN 1993-1-5:2006, "Eurocode 3: Design of steel structures Part 1-5: Plated structural elements," British Standards Institution, London, 2006.
- [41] EN 1993:1-1, "Eurocode 3: Design of steel structures Part 1-1: General rules," European Committee for Standardization, Brussels, 2005.
- [42] H.-m. Chan, Y. Wang, K. Zhou, D. Lam, W. Guo, L. Li, A. Ajayebi and P. Hopkinson,
- "Reclaiming structural steels from the end of service life composite structures for reuse An assessment of the viability of different methods," *Developments in the Built Environment,* vol. 10, no. 100077, 2022, doi: 10.1016/j.dibe.2022.100077
- [43] BS EN 10025-2:2004, "Hot rolled products of structural steels Part 2: Technical delivery conditions for non-alloy structural steels," Europen Committee for Standardization, Brussels, 2004.